

Available Now R&D Systems 2010 Catalog

Offering more than 15,000 Quality Products

Click here to request your copy today

R&D  
SYSTEMS®

## The Journal of Immunology

This information is current as  
of January 23, 2010

# Development of a Novel Noncompetitive Antagonist of IL-1 Receptor

Christiane Quiniou, Przemyslaw Sapieha, Isabelle Lahaie,  
Xin Hou, Sonia Brault, Martin Beauchamp, Martin Leduc,  
Lenka Rihakova, Jean-Sébastien Joyal, Sylvain Nadeau,  
Nikolaus Heveker, William Lubell, Florian Sennlaub,  
Fernand Gobeil, Jr., Greg Miller, Alexey V. Pshezhetsky  
and Sylvain Chemtob

*J. Immunol.* 2008;180:6977-6987

<http://www.jimmunol.org/cgi/content/full/180/10/6977>

### References

This article **cites 87 articles**, 27 of which can be accessed free at:  
<http://www.jimmunol.org/cgi/content/full/180/10/6977#BIBL>

1 online articles that cite this article can be accessed at:  
[http://www.jimmunol.org/cgi/content/full/180/10/6977#otherarti  
cles](http://www.jimmunol.org/cgi/content/full/180/10/6977#otherarticles)

### Subscriptions

Information about subscribing to *The Journal of Immunology* is  
online at <http://www.jimmunol.org/subscriptions/>

### Permissions

Submit copyright permission requests at  
<http://www.aai.org/ji/copyright.html>

### Email Alerts

Receive free email alerts when new articles cite this article. Sign  
up at <http://www.jimmunol.org/subscriptions/etoc.shtml>

*The Journal of Immunology* is published twice each month by  
The American Association of Immunologists, Inc., 9650  
Rockville Pike, Bethesda, MD 20814-3994.  
Copyright ©2008 by The American Association of  
Immunologists, Inc. All rights reserved.  
Print ISSN: 0022-1767 Online ISSN: 1550-6606.



# Development of a Novel Noncompetitive Antagonist of IL-1 Receptor<sup>1</sup>

Christiane Quiniou,\* Przemyslaw Sapieha,\* Isabelle Lahaie,\* Xin Hou,\* Sonia Brault,\* Martin Beauchamp,\* Martin Leduc,\* Lenka Rihakova,\* Jean-Sébastien Joyal,\* Sylvain Nadeau,\* Nikolaus Heveker,\* William Lubell,<sup>†</sup> Florian Sennlaub,<sup>¶</sup> Fernand Gobeil, Jr.,<sup>§</sup> Greg Miller,<sup>‡</sup> Alexey V. Pshezhetsky,\* and Sylvain Chemtob<sup>2\*</sup>

**IL-1 is a major proinflammatory cytokine which interacts with the IL-1 receptor I (IL-1RI) complex, composed of IL-1RI and IL-1R accessory protein subunits. Currently available strategies to counter pathological IL-1 signaling rely on a recombinant IL-1 receptor antagonist, which directly competes with IL-1 for its binding site. Presently, there are no small antagonists of the IL-1RI complex. Given this void, we derived 15 peptides from loops of IL-1R accessory protein, which are putative interactive sites with the IL-1RI subunit. In this study, we substantiate the merits of one of these peptides, rytvela (we termed "101.10"), as an inhibitor of IL-1R and describe its properties consistent with those of an allosteric negative modulator. 101.10 (IC<sub>50</sub> ≈ 1 nM) blocked human thymocyte proliferation in vitro, and demonstrated robust in vivo effects in models of hyperthermia and inflammatory bowel disease as well as topically in contact dermatitis, superior to corticosteroids and IL-1ra; 101.10 did not bind to IL-1RI deficient cells and was ineffective in vivo in IL-1RI knockout mice. Importantly, characterization of 101.10, revealed noncompetitive antagonist actions and functional selectivity by blocking certain IL-1R pathways while not affecting others. Findings describe the discovery of a potent and specific small (peptide) antagonist of IL-1RI, with properties in line with an allosteric negative modulator. *The Journal of Immunology*, 2008, 180: 6977–6987.**

**O**f the numerous factors involved in inflammatory conditions, compelling evidence points to a dominant contribution by IL-1, a 17-kDa cytokine, in acute bouts of inflammation (1). A role for IL-1 has been clinically validated in a number of chronic inflammatory diseases such as rheumatoid arthritis (2), inflammatory bowel disease, and strongly suggestive in osteoarthritis and psoriasis (3). IL-1 interplays with a number of other important mediators of inflammation, such as TNF, IL-18, and IL-6. IL-1 exerts its biological effects by interacting with the IL-1 receptor type I (IL-1RI),<sup>3</sup> which is composed of a ligand-binding subunit and a signaling subunit (named the IL-1R accessory protein (IL-1RacP)); IL-1RII (membrane-bound and soluble)

is an inhibitory type receptor of IL-1RI (4). Stimulation of IL-1RI leads to activation of various downstream signaling mediators, notably PGE<sub>2</sub> and NF-κB, which partake in conveying hyperthermic and proinflammatory effects of IL-1 (5).

Presently, a recombinant protein of the natural IL-1 receptor antagonist (IL-1ra) (–17.5 kDa; Kineret) is the only clinically effective approach to interfere specifically in a competitive manner with IL-1 actions; regrettably, its administration is associated with a number of undesirable adverse effects and limited efficacy (6). IL-1ra selectively targets IL-1 by competing with the latter for receptor binding.

Alternatively, targeting IL-1RI with small inhibitors would be advantageous in that it would be potentially simpler to administer, could be effective transepithelially, be hopefully devoid of adverse effects, and be less costly. Such a compound would be further beneficial if it exhibited noncompetitive properties (and possibly functional selectivity as an allosteric modulator, which would not abolish all functions of IL-1RI (7)); but this has yet to be achieved (5).

The concept that peptides that reproduce the sequence of specific regions of receptors (or enzymes) can interfere with actions of these proteins of interest has been amply documented (8–14). Loop regions of receptors (and other proteins) are particularly relevant in this context as they affect appropriate conformation and/or interactions with other subunits and partners (15); this notion also applies to different loops of IL-1RacP that interact with the IL-1RI subunit (16). For example, D-peptides (more active and stable than L-peptides (10)) derived from transmembrane and dimerization domains respectively of β-adrenergic and vascular endothelium growth factor receptors hinder dimerization (13, 17); similarly, a peptide fragment retaining a motif of the β-amyloid interferes with assembly of this protein into plaques (10). Because regions targeted by these molecules do not need to arise from the ligand-binding site,

\*St.-Justine Hospital Research Centre, Montreal; <sup>†</sup>Department of Chemistry, University of Montreal, Montreal; <sup>‡</sup>Department of Pharmacology and Therapeutics, McGill University, Montreal, Quebec; <sup>§</sup>Department of Pharmacology, University of Sherbrooke, Sherbrooke, Quebec, Canada; and <sup>¶</sup>Institut National de la Santé et de la Recherche Médicale, U872, Paris, France

Received for publication June 12, 2007. Accepted for publication March 11, 2008.

The costs of publication of this article were defrayed in part by the payment of page charges. This article must therefore be hereby marked *advertisement* in accordance with 18 U.S.C. Section 1734 solely to indicate this fact.

<sup>1</sup> This work was supported in part by grants from Valorisation Recherche Québec and the Canadian Institute of Health Research. S.C. is recipient of a Canada Research Chair in perinatology. N.H. is the recipient of a Scientist Award from the Canadian Institute of Health Research. C.Q., P.S., S.B., M.B., M.L., and J.-S.J. are recipients of fellowships/studentships from the Heart and Stroke Foundation of Canada (to C.Q., P.S., and M.L.), Canadian Institutes of Health Research (to S.B. and M.B.), and the Canadian Child Health Clinician Scientist Program-Canadian Institutes of Health Research (to J.-S.J.).

<sup>2</sup> Address correspondence and reprint requests to Dr. Sylvain Chemtob, St.-Justine Hospital Research Centre, University of Montreal, 3175 Cote-Ste-Catherine, Montreal, Quebec, H3T 1C5 Canada. E-mail address: sylvain.chemtob@umontreal.ca

<sup>3</sup> Abbreviations used in this paper: IL-1RI, IL-1 receptor type I; IBD, inflammatory bowel disease; BP, blood pressure; TNBS, 2,4,6-trinitrobenzenesulfonic acid; MBP, mean BP.

Copyright © 2008 by The American Association of Immunologists, Inc. 0022-1767/08/\$2.00

these peptides would conceivably often exhibit allosteric modulatory properties (18, 19). Allosterism can alter signaling modalities (18) and down-stream responses without completely inhibiting receptor function (7), and thus confer greater selectivity. This has, for instance, been shown for thiochrome, a selective allosteric enhancer of the M4 muscarinic receptor (19), for TNF- $\alpha$ -RI (20), and for adhesion molecules such as the LFA-1 integrin of lymphocytes where a peptide binds to an allosteric site and interferes with some (but not all) of its function (21).

Along these lines, in relevance to IL-1R, it has recently been demonstrated that a recombinant of the major extracellular portion of the IL-1RacP (~75 kDa) exhibits *in vivo* efficacy in a model of autoimmune arthritis without interfering with all actions exerted by IL-1RI (22). On the basis of the overall rationale presented above, we generated peptides derived from extracellular loops and interdomain regions of IL-1RacP and screened them against IL-1-induced effects. We hereby describe for the first time 101.10 (rytvela), a small selective peptidic antagonist of IL-1RI, which exhibits properties consistent with those of an allosteric modulator, and is effective in models of acute inflammation.

## Materials and Methods

### Animals, cells, and peptides

Animals were used according to a protocol of the Animal Care committee of Hôpital Ste-Justine along with the principles of the Canadian Council on Animal Care. Sprague-Dawley rats and CD-1 mice were obtained from Charles River Laboratories. *Il1r* gene knockout ( $^{-/-}$ ) mice generated on the B6129S1-*Il1r*<sup>tm/Rom1</sup>/J background and corresponding wild-type control B6129SF2/J strain were purchased from Jax Mice Laboratories (23). Human thymocyte TF-1 cells were obtained from American Type Culture Collection. All D-peptides were custom synthesized by Sigma-Aldrich (>96% purity).

### Peptide design

Regions of the IL-1R accessory protein were identified based on crystallography and modeling data (16, 24), which were supported by hydrophobic and flexibility profiles, as well as homology domains using computational analysis (ProDom (25), PROSITE (26), Predict Protein (26), and ProtScale (27)). Fifteen corresponding homologous peptides (all D-octadeca, sense (NH<sub>3</sub>-COOH) and anti-sense (COOH-NH<sub>3</sub>)) were derived from primary sequences of extracellular regions (loops and interdomain regions) of the IL-1RacP regions.

### IL-1-induced hyperthermia

Sprague-Dawley rats (300–330 g) were anesthetized with 2% isoflurane and placed under a radiant warmer to maintain core (rectal) temperature at ~37.5°C. A polypropylene tube (PE-90) was inserted in the jugular vein for injections. The femoral artery was catheterized (PE-90) to collect blood samples. The probe of an electronic thermometer was inserted ~4 cm into the rectum to measure temperature. 101.10 (1 mg/kg; estimated concentration in maximum efficacy range (~200 nM); see Fig. 2), Ibuprofen (40 mg/kg) or vehicle (normal saline) was injected 10 min before IL-1 $\beta$  (5  $\mu$ g/kg). Rectal temperature was measured at different time points thereafter.

For arterial blood pressure (BP) measurements, LPS (LPS; 10 mg/kg) was injected *i.p.* 20 min before 101.10 (1 mg/kg, *ip*) in wild-type and IL-1R $^{-/-}$  B6129S mice; the left carotid artery was catheterized with a polyethylene PE-10 catheter and BP was recorded using a Statham pressure transducer connected to a Gould recorder. BP measurement variations were recorded for an hour.

For intracerebroventricular injections, a burr hole was drilled through the skull 1.5 mm lateral to the midline and 1.2 mm posterior to the bregma on the right side. A 10-mm 20-gauge stainless steel hypodermic blunt needle was inserted 4–4.5 mm below the surface of the skull into the right lateral ventricle and secured to the skull with acrylic cement (28); EP<sub>3</sub> agonist M&B28767 was injected. The jugular vein was exposed as above. Animals were pretreated with 101.10 (1 mg/kg *i.v.*) and administered intracerebroventricularly with an EP<sub>3</sub> agonist M&B28767 (2  $\mu$ l of 1  $\mu$ M solution; estimated concentration of 50 nM for cerebroventricular volume ~40  $\mu$ l (29)). Rectal temperature was monitored as described above.

### Trinitrobenzene sulfonic acid-induced model of inflammatory bowel disease

The efficacy of 101.10 was tested on a model of colon inflammation induced by 2,4,6-trinitrobenzenesulfonic acid (TNBS). TNBS was administered intrarectally to Sprague-Dawley rats anesthetized with 2% isoflurane (30, 31). In brief, 120 mg/ml TNBS dissolved in 50% ethanol (vol/vol) was injected into the rectum/sigmoid colon (8 cm from anus) (total volume of 0.25 ml per rat; 30 mg total) via a polyethylene tubing (PE50). The control rat received 0.25 ml of vehicle (normal saline). Dexamethasone (0.75 mg/kg/day) (32), IL-1Ra (8 mg/kg/day) (33), and infliximab (10 mg/kg/day) (34) were injected *i.p.* (within 15 min of TNBS) once a day, and 101.10 (1 mg/kg/day) twice a day. Some animals were also treated with intrarectal 101.10 (1 mg/kg/day) to assess its efficacy upon local application to epithelium (which could also be of clinical interest).

Forty eight hours after administration of TNBS, rats were euthanized by CO<sub>2</sub> inhalation and colon removed and assessed for macroscopic observations (abdominal adhesions, faecal consistency, ulcerations, and discoloration). Tissue was then rolled over ~10 cm length along its transverse axis, fixed, and cut for histology; this enabled histological evaluation in the same tissue over a reasonable length (damage to surface epithelium, crypt distortion, and ulcerations, neutrophil infiltration). Tissues were stained with hematoxylin and phloxin. Tissue injury was evaluated macroscopically and microscopically by three investigators blinded to treatment assignments, based on an adapted version of Peterson's scale (30); mean of scores was calculated for each animal.

Tissue neutrophil invasion was assessed by myeloperoxidase assay. Myeloperoxidase activity was determined as reported (35). In brief, tissue specimens (200–400 mg) were homogenized three times (30 s, 4°C) in 50 mM phosphate buffer (pH 6.0) with 0.5% hexadecyltrimethylammonium bromide, sonicated for 10 s, and exposed to three freeze-thaw cycles. Samples were centrifuged at 20,000  $\times$  g for 20 min. A total of 100  $\mu$ l supernatant was diluted in 2.9 ml of 50 mM potassium phosphate buffer (pH 6.0) containing 526  $\mu$ M of *O*-dianisidine hydrochloride. Enzymatic reaction was started with the addition of 0.0005% of peroxide. Myeloperoxidase activity was calculated by dividing the absorbance (460 nm at 25°C) change per min (total 5 min) with the extinction coefficient for *O*-dianisidine ( $\epsilon = 1.13 \times 10^4$  M<sup>-1</sup>cm<sup>-1</sup>), and was normalized to protein concentration; 1 unit myeloperoxidase activity was defined as that degrading 1  $\mu$ mol of peroxide per min at 25°C. Values were presented as percent of those in TNBS-injected vehicle-treated (control) rats.

Wright stain was used for histological confirmation of inflammatory cell infiltration into tissues. Intestinal sections were mounted on slides covered with 750  $\mu$ l of Wright staining solution (Fluka) for 1 min, covered with 1.5 ml of distilled water for 2 min and finally washed with distilled water and mounted with Gel/Moun (Biomedica). Digital images of intestine were obtained (Nikon DXM 1200). Intestine total length and intact villi were measured with the Image-Pro Plus software (5.1 version). The percentage of intact villi was evaluated by dividing the length of intact villi by the total intestinal length (36).

T lymphocytes were counted on intestinal sections incubated for 2 h at room temperature with anti-CD4 Ab (mouse anti-rat CD4; US Biological) diluted in PBS containing 0.4% Triton X-100 (Sigma-Aldrich), 1% BSA (fraction V; MP Biomedicals), and counterstained with a tagged secondary Ab (goat anti-mouse IgG; Molecular Probes). Intestinal sections were mounted and positive T cells counted (per mm<sup>2</sup>) on digitized images as reported (37).

### Phorbol myristate acetate-induced dermatitis

The efficacy of 101.10 (applied topically) was assessed in a model of cutaneous inflammation induced with 0.05% PMA in acetone applied to ears of CD-1 mice, *Il1r* knockout mice, and wild-type congeners B6129S (38). PMA was applied to both ears, while one ear was treated 45 min after PMA with 20  $\mu$ l of different concentrations of 101.10 in PEG-400. Ear thickness was measured with a caliper. Forty two hours after the start of treatment, Evans blue dye was injected intracardiac to determine capillary extravasation (see below), and 4 mm ear punches made and weighed. Ear punches were then minced and incubated in dimethyl formamide at 80°C for 3 h. Supernatant was centrifuged and absorbance measured at 620 nm with a background correction of 740 nm (39, 40), and normalized for tissue weight; concentration was determined from Evan's blue standard curve. PGE<sub>2</sub> was also measured in the tissue (see below).

### Western blots

Western blots of p38, phospho-p38, JNK, phospho-JNK, Erk1/2, phospho-Erk1/2, I $\kappa$ B, phospho-I $\kappa$ B, and IL-1R were performed as previously described (41). Essentially rat thymocytes or microvascular endothelial cells

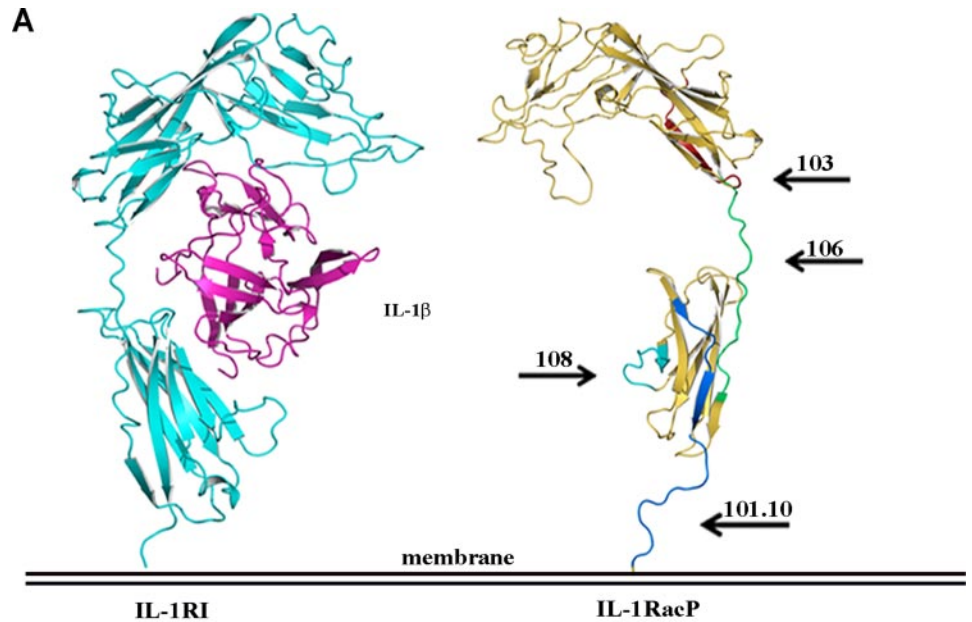


**FIGURE 1.** A, Ribbon-like model of IL-1RI (1ITB), IL-1, and IL-1RacP and identification of regions of derived effective peptides. B, Primary sequence of the IL-1RacP. Colored sequences refer to corresponding loops indicated on A; blue, 101.10, turquoise: 108, green, 106, red, 103.

**B Sequence of the extracellular/transmembrane portion of IL-1RacP: targeted loops/regions are color indicated**

```

1  MTLWCVVSL YFYGILQSDA SERCDDWGLD TMRQIQVFED EPARIKCPLE EHFLKFNYST 60
61 AHSAGLTLIW YWTRQDRDLE EPINFRLPEN RISKEKDLVW FRPTLLNDTG NYTCMLRNTT 120
121 YCSKVAFPLE VVQKDFSCFNS PMKLPVHKLY IEYGIQRITC PNVGDFPSS VKPTITWYMG 180
181 CYKIQNFNNV IPEGMNLNFL IALISNNGNY TCVVTYPENG RTFHLTRILT VKVVGSPKNA 240
241 VPPVIHSPND HVVYEKEPGE ELLIPTVYF SFLMDSRNEV WWTIDGKKPD DITIDVTINE 300
301 SISHSRTEDE TRTQILSIKK VTSEDLKRSY VCHARSAKGE VAKAAKVKQK VPAPRYTVEL 360
361 ACGFGATVLL VVILIVVYHV YWL 383
    
```

(transmembrane region)

were preincubated (45 min) at 37°C with the peptide 101.10 (10<sup>-7</sup>M), followed by 30 min incubation with IL-1β 50 pM, IL-6 (0.5 ng/ml), or IL-18 (100 ng/ml). Cells were then lysed, run on 12% SDS-PAGE, and immunoblots were revealed with specific Abs (Calbiochem, Santa Cruz, Cell Signaling) of total and phosphorylated proteins.

**[<sup>3</sup>H]thymidine incorporation**

Cell proliferation was assessed by incorporation of [<sup>3</sup>H]thymidine as we described (42). Essentially human TF-1 cells were cultured in complete RPMI supplemented with GM-CSF (2 ng/ml; BD Biosource). Cells were deprived of growth factors for 18 h before preincubation with 101.10 followed by treatment with IL-1β (1 ng/ml). For IL-1β dose-response curves and Schild Plot conversion, cells were preincubated with a constant concentration of 101.10 and different concentrations of IL-1β. After 24 h [<sup>3</sup>H]thymidine (1 μCi/well; Amersham) was added for another 24 h. Cells were harvested, washed four times with PBS (10 mM Na<sub>2</sub>HPO<sub>4</sub>, 2 mM KH<sub>2</sub>PO<sub>4</sub>, 137 mM NaCl, 2.7 mM KCl; pH 7.4) and lysed with 0.1 N NaOH/0.1% Triton-X100. Radioactivity was measured (Beckman Multi-Purpose Scintillation Coulter Counter LS6500).

**PGE<sub>2</sub> concentrations**

PGE<sub>2</sub> was measured in cell cultures, plasma, and tissues as we described in detail (43). TF-1 cells were preincubated 45 min at 37°C with different concentrations of peptides or 9 nM of IL-Ra, after which IL-1β (50 pM) was added to the medium. After 24-h incubation, PGE<sub>2</sub> was measured on

growth medium. Measurement of PGE<sub>2</sub> in tissues and plasma was performed as follows. Ears were homogenized in cold indomethacin (10 μM)-containing buffer, whereas plasma was collected in EDTA- and indomethacin (10 μM)-containing tubes; both were passed through C18 columns after which PGE<sub>2</sub> was measured by radioimmunoassay (Amersham).

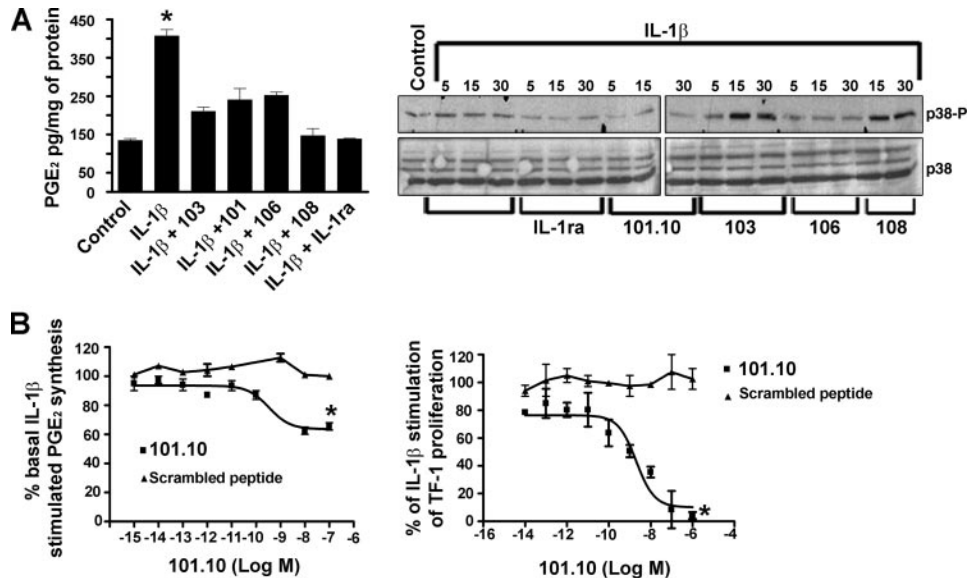
**Radiolabelled ligand binding**

Radiolabelled binding of cytokines was performed as comparably described (44, 45). Freshly isolated rat thymocytes (10<sup>6</sup>) were suspended in binding buffer (PBS, HEPES 10 mM, 0.02% Na<sub>2</sub>S<sub>2</sub>O<sub>8</sub>, 0.05% gelatin, and preincubated (20 min) with increasing concentrations of nonradiolabelled IL-1β or 101.10 followed by incubation with [<sup>125</sup>I]IL-1β for 2 h at room temperature. Similarly, thymocytes were preincubated (20 min) with 101.10 (10<sup>-1</sup>-10<sup>-6</sup> M), after which [<sup>125</sup>I]101.10 (6 and 60 nM) was added. For saturation isotherms, freshly isolated thymocytes from B6129S wild-type and IL-1RI knockout (-/-) mice were incubated with different concentrations of [<sup>125</sup>I]101.10 (1 h) with and without a 1000-fold excess unlabelled peptide to determine specific binding for each concentration of [<sup>125</sup>I]101.10; reaction volume was 100 μl at 37°C. Cells were washed four times with PBS buffer and lysed with 0.1 N NaOH/0.1% Triton X-100. Bound radioactivity was measured on cell lysates with a Packard Cobral autogamma counter. Affinity and inhibitory constants were determined using the GraphPad Prism 4 software. To ascertain binding profiles performed in thymocytes (low number of IL-1-binding sites (46, 47), experiments were also conducted on NIH3T3 cells (~5800 IL-1-binding sites/cell).

Table I. Sequence of peptides and targeted regions of the extracellular portion of the accessory protein

Peptide Assigned No.	Peptide Sequences (Sense)	IL-1RacP Target Loops Sequences	IL-1RacP Regions Targeted
101.10	NH <sub>2</sub> -rytvela-COOH	NH <sub>2</sub> -VAKAAKVKQKVPAPRYTVELAC-COOH	D3-juxtamembranous
103	NH <sub>2</sub> -mklpvkhly-COOH	NH <sub>2</sub> -PMKLPVHKLYIEY-COOH	Loop D1-D2
106	NH <sub>2</sub> -vgspknavppv-COOH	NH <sub>2</sub> -VKVVGSPKNAVPPVIHSPND-COOH	Loop D2-D3
108	NH <sub>2</sub> -wtldgkdpddl-COOH	NH <sub>2</sub> -WWTIDGKKPDDI-COOH	Loop in D3

**FIGURE 2.** In vitro efficacy of IL-1RacP-derived peptides. *A*, Effects of peptides (0.1  $\mu$ M) and IL-1ra (9 nM) on IL-1 (50 pM)-induced PGE<sub>2</sub> formation and p38 phosphorylation on human TF-1 cells. *Top gels* represent phosphorylated p38 and *bottom gels* represent total p38. Value on top of p38 gels refer to time (min). Values are mean  $\pm$  SEM of three experiments each performed in duplicate; \*,  $p < 0.01$  compared with IL-1-induced. *B*, Dose response of 101.10 and scrambled peptide (verlyta) on IL-1 (1 ng/ml)-induced PGE<sub>2</sub> synthesis and cell proliferation in human TF-1. Values are mean  $\pm$  SEM of 8 experiments each performed in duplicate; \*,  $p < 0.01$  compared with scrambled peptide or  $10^{-3}$  M 101.10 concentration (ANOVA).



Binding of [<sup>125</sup>I]101.10 to IL-1R-expressing cells was confirmed by cross-linking. IL-1R-expressing and -deficient thymocytes (10<sup>6</sup>) were prepared as described above with [<sup>125</sup>I]101.10 (100 nM) in absence or presence of 1 and 10  $\mu$ M unlabelled 101.10 for 45 min at 37°C (ascertaining equilibrium for peptide binding). The nonpermeable cross-linker (Bis(sulfosuccinimidyl)suberate [BS3]; 11 Å) was then added to a final concentration of 2.5 mM and samples were incubated at 4°C for 30 min to minimize active internalization of BS3 (48) (Pierce). The reaction was quenched with 20 mM Tris pH 7.5 for 15 min at room temperature. Cells were centrifuged at 4000 rpm for 10 min, lysed for 30 min on ice (150  $\mu$ l of lysis buffer), and electrophoresed on SDS-PAGE under nonreducing conditions. Autoradiography and Western Blot analysis with anti-IL-1R Ab were then performed.

#### Data analysis

Results were analyzed by one- or two-way ANOVA factoring for concentration or treatments. Postanova comparisons among means were performed using the Tukey-Kramer method. Statistical significance was set at  $p < 0.05$ . Data are presented as mean  $\pm$  SEM.

## Results

### Peptides and screening of efficacy

Using the rationale presented above regarding intramolecular peptides that interfere with actions of the protein of interest (8–14) we identified extracellular regions of the IL-1RacP reported to interact with IL-1RI subunit (1ITB). Fifteen corresponding homologous peptides (all D-octa-deca, sense (NH<sub>3</sub>-COOH) and anti-sense (COOH-NH<sub>3</sub>)) were designed based on crystallography and modeling data (16, 24), which were supported by hydrophobic and flexibility profiles as well as homology domains using computational analysis (ProDom (25), PROSITE (26), Predict Protein (26), ProtScale (27)); BLAST analysis was coherent with selectivity of peptides for IL-1RacP. IL-1RacP regions chose exhibited interspecies homology for human, rat, and mouse. Screening of peptide efficacy was performed on IL-1-induced PGE<sub>2</sub> formation. Four of the peptides (termed 103, 106, 108, and 101.10 (all D-)); 0.1  $\mu$ M derived from regions of the IL-1RacP depicted in Fig. 1 and presented in Table I effectively inhibited PGE<sub>2</sub> formation to varying degrees (Fig. 2A). Interestingly, IL-1-induced p38 phosphorylation was only inhibited by 101.10 (rytvela) and as expected by human recombinant IL-1ra (Fig. 2A); whereas 103 and 108 increased p38 phosphorylation, and 106 was ineffective, consistent with possible allosteric modulation of receptor signaling by 103, 106, and 108 (16, 49). Because 101.10 was reproducibly

effective even in inhibiting IL-1-induced I $\kappa$ B phosphorylation (data not shown) and exhibited high potency (see below), we decided to focus and further characterize this small heptapeptide (0.8 kDa).

### Efficacy and potency of 101.10

Compilation of data reveals that 101.10 inhibited dose-dependently IL-1-induced PGE<sub>2</sub> formation (IC<sub>50</sub> = 0.5 nM; Emax  $\approx$  50%, consistent with screening) and IL-1-induced human thymocyte (TF-1 cell) proliferation (IC<sub>50</sub> = 2 nM; Emax  $\geq$  90%) (Fig. 2B). Similar

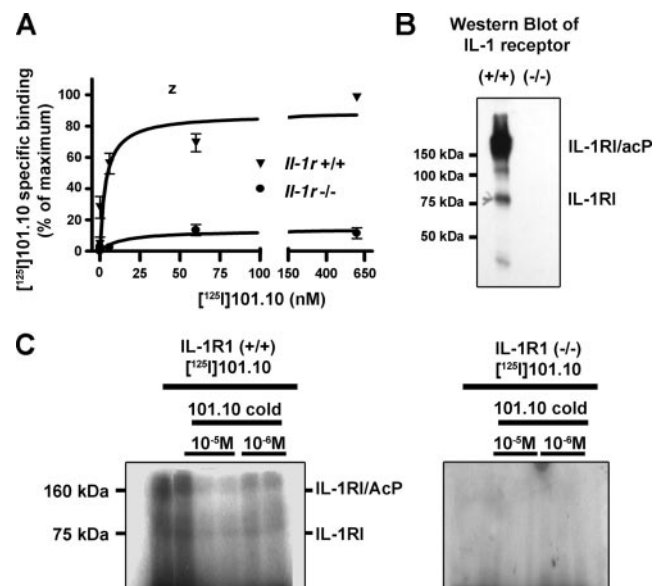
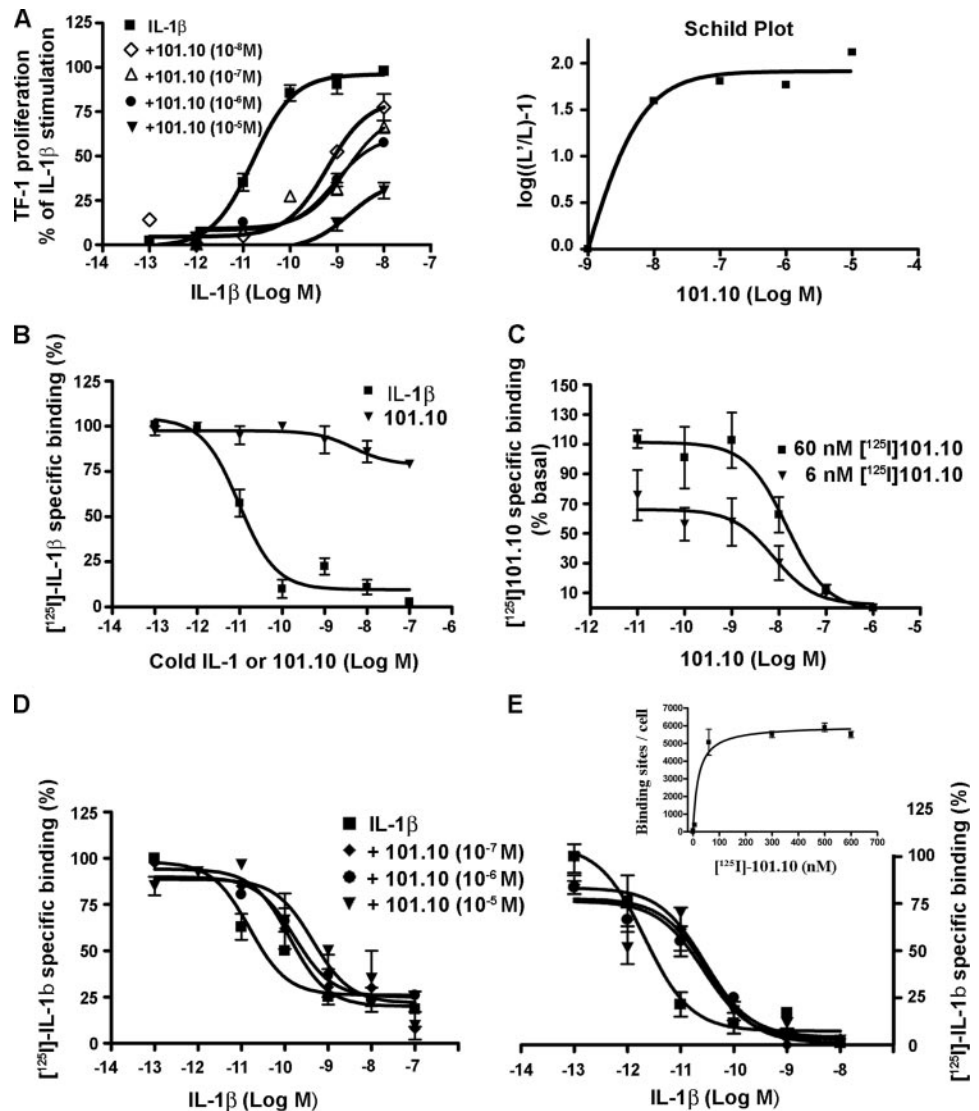


**FIGURE 3.** Binding of [<sup>125</sup>I]101.10. *A*, Saturation isotherm of [<sup>125</sup>I]101.10 in thymocytes from wild-type and IL-1RI<sup>-/-</sup> mice. Values are mean  $\pm$  SEM of percent of maximum binding in three experiments each performed in duplicate. *B*, Western blot of IL-1R in thymocytes from wild-type and IL-1RI<sup>-/-</sup> animals. *C*, Representative (of  $n = 3$ ) autoradiogram of electrophoresed (nonreducing conditions) [<sup>125</sup>I]101.10 (100 nM)-bound cells following chemical cross-linking of IL-1RI-expressing (+) and IL-1RI-devoid (-) thymocytes using the 11 Å BS3 crosslinker; superimposition of immunoblot for IL-1RI reveals full IL-1RI and its subunit(s) in IL-1RI-expressing cells, and totally clear autoradiogram in IL-1RI-devoid cells.

**FIGURE 4.** Noncompetitive effects of 101.10. *A*, Dose-response of 101.10 on IL-1-induced TF-1 cell proliferation, and Schild plot conversion; note plateaued curve indicative of noncompetitive action of 101.10. Values are mean of triplicate experiments. *B*, Displacement of bound [ $^{125}$ I]IL-1 (25 pM) by IL-1 or 101.10 in rodent thymocytes; values are mean  $\pm$  SEM of six experiments each performed in triplicate. *C*, Displacement of [ $^{125}$ I]101.10 by (unlabelled) 101.10 at two different initial concentrations of [ $^{125}$ I]101.10;  $K_i = 4$  nM. *D*, Displacement of bound [ $^{125}$ I]IL-1 (25 pM) by IL-1 in the presence of increasing concentrations of 101.10 in rodent thymocytes. *E*, Displacement of bound [ $^{125}$ I]IL-1 (25 pM) by IL-1 in the presence of increasing concentrations of 101.10 in NIH3T3 cells; insert reveals 101.10 binding sites/cell in NIH3T3 cells. *D* and *E*, Note the right shift of displacement curves by 101.10. For *C–E*, values are mean  $\pm$  SEM of three experiments each performed in duplicate.



effects were observed in a different IL-1-responsive cell type, specifically microvascular endothelial cells; scrambled peptide (very-tla) was ineffective.

[ $^{125}$ I]101.10 bound specifically in a saturable manner with an affinity constant ( $K_D$ ) of 5 nM only to thymocytes containing IL-1RI (from wild-type animals) but hardly to those from *Il-1r<sup>-/-</sup>* animals (Fig. 3, *A* and *B*). Binding of [ $^{125}$ I]101.10 to IL-1RI-expressing thymocytes using 11 Å BS3 cross-linker was confirmed by autoradiogram; immunoblot overlay coincided with IL-1RI and IL-1RI/IL-1RacP complex (nonreducing conditions; Fig. 3C); more importantly, no [ $^{125}$ I]101.10 cross-linking was detected on autoradiogram in cells devoid of IL-1RI.

We next determined whether effects of 101.10 inhibited IL-1-induced TF-1 cell proliferation in a competitive or noncompetitive manner. TF-1 cell proliferation was studied in cells pretreated with different concentrations of 101.10 in presence of increasing concentrations of IL-1. 101.10 diminished maximum TF-1 proliferation induced by IL-1 with an estimated  $pA_2$  value of 5 nM (101.10 concentration needed to double  $EC_{50}$ ), and augmented in a saturable manner its  $EC_{50}$  by 100-fold; accordingly, a plateaued Schild plot was detected (Fig. 4A), indicative of noncompetitive effects of 101.10 on IL-1-induced effects. In line with these observations, 101.10 marginally displaced bound [ $^{125}$ I]IL-1 (Fig. 4B); consistently, bound [ $^{125}$ I]101.10 was displaceable by (unlabelled) 101.10

(inhibitory constant  $K_i = 4$  nM) (Fig. 4C), but hardly by IL-1 (data not shown). Importantly, 101.10 diminished IL-1-binding affinity by increasing the  $K_i$  (on [ $^{125}$ I]IL-1-prebound cells) by  $\sim$ 13–16-fold in thymocytes (Fig. 4D) as well as in NIH3T3 which contain  $\sim$ 5500 101.10-binding sites/cell (8% nonspecific binding) (Fig. 4E); this strongly suggested that 101.10 modulated IL-1-binding affinity.

#### Selectivity of 101.10

Selectivity of 101.10 was further tested on effects of homologous cytokine of the IL-1 family, namely IL-18, as well as on other proinflammatory cytokines such as IL-6. IL-18-induced respectively TNF- $\alpha$ - and LPS-dependent JNK and p38 phosphorylation were unaffected by 101.10 (Fig. 5A). Likewise, IL-6-induced Erk1/2 phosphorylation was unaltered by 101.10 (Fig. 5A).

IL-1 causes hyperthermia via formation of PGE $_2$  that in turn activates its EP $_3$  receptor (50, 51). We tested whether this effect can be attenuated by 101.10. IL-1 caused a  $\sim$ 1°C increase in core temperature associated with a rise in PGE $_2$  plasma levels (Fig. 5B). 101.10 (1 mg/kg; estimated concentration in maximum efficacy range ( $\sim$ 200 nM)) markedly diminished IL-1-induced peak hyperthermia and attenuated the associated rise in plasma PGE $_2$  in rat (Fig. 5B). As expected the prostaglandin synthase inhibitor ibuprofen (40 mg/kg, as we have shown to inhibit PGE $_2$  formation

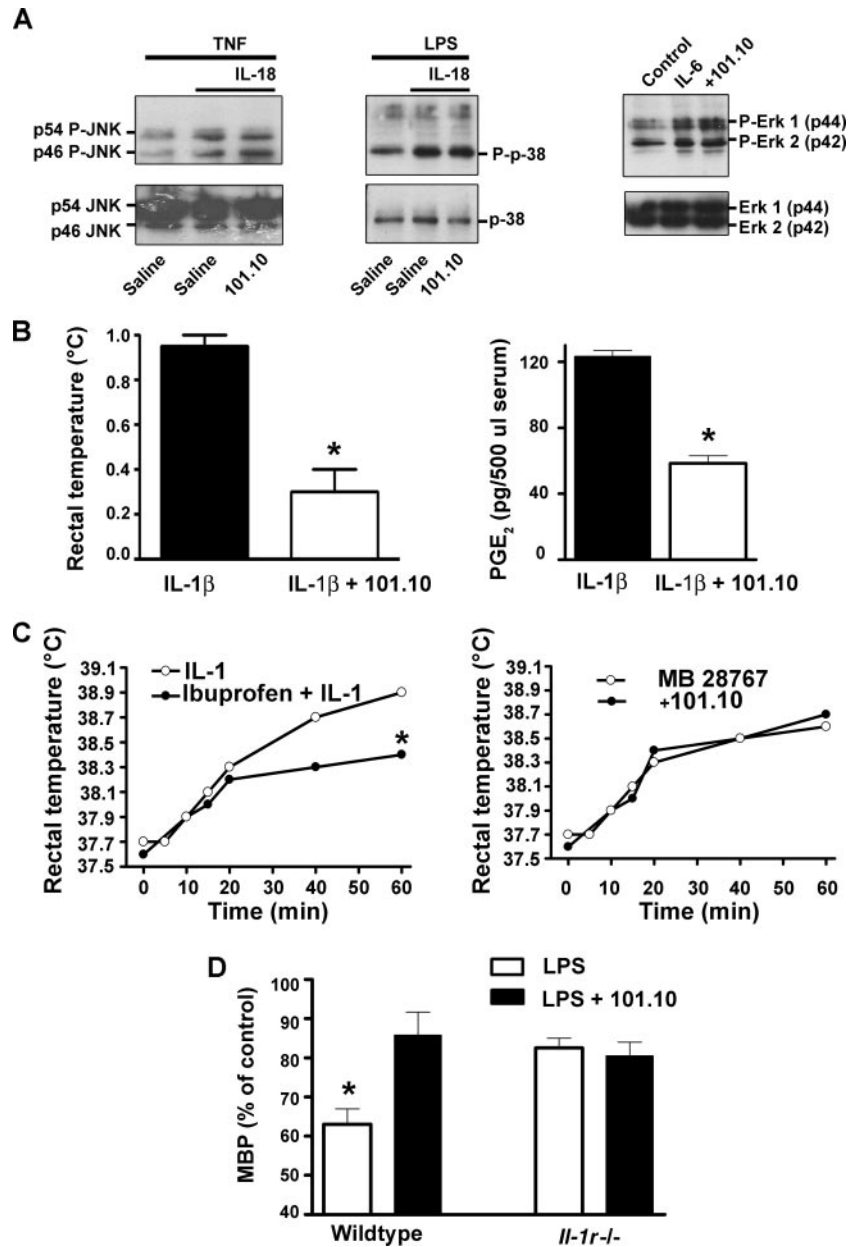


**FIGURE 5.** Selectivity of 101.10. *A*, Effects of TNF- $\alpha$  (1 ng/ml)- and LPS (LPS; 5  $\mu$ g/ml)-dependent IL-18-induced (100 ng/ml) JNK and p38 phosphorylation in microvascular endothelial cells (EC) in absence or presence of 101.10 (1  $\mu$ M); preincubations with TNF- $\alpha$  and LPS enhance IL-18 receptor expression. Effects of IL-6 (0.5 ng/ml) in EC cells in absence or presence of 101.10 (1  $\mu$ M). Blots are representative of three experiments. *B*, Effects of 101.10 on IL-1-induced hyperthermia and plasma PGE<sub>2</sub> concentrations in rat (101.10 1 mg/kg iv) and IL-1 (5  $\mu$ g/kg iv). *C*, Effect of 101.10 on EP<sub>3</sub>-selective PGE<sub>2</sub> analog M&B28767-induced hyperthermia. *Left panel*, Inhibition of IL-1- (5  $\mu$ g/kg iv) induced hyperthermia by prostaglandin synthase inhibitor ibuprofen (ibu; 40 mg/kg iv) ascertains role of prostaglandins. *Right panel*, Intracerebroventricular injection of M&B28767 (2  $\mu$ l of 1  $\mu$ M solution; estimated concentration of 50 nM for cerebroventricular volume  $\sim$ 40  $\mu$ l (29) causes a comparable hyperthermia, which is unaltered by 101.10. *D*, Effects of 101.10 (1 mg/kg ip) on LPS-induced maximum hypotension (10 mg/kg ip) in wild-type and *IL-1RI*<sup>-/-</sup> mice. 101.10 significantly attenuated LPS-induced hypotension in wild-type but not in *IL-1RI*<sup>-/-</sup> mice; note that effects of LPS in *IL-1RI*<sup>-/-</sup> are nearly identical with those in 101.10-treated wild-type animals. Values for *B–D* are mean  $\pm$  SEM of two to five experiments; \*, *p* < 0.05 compared with IL-1 alone (*B* and *C*) or other corresponding values without asterisks (*D*; ANOVA).

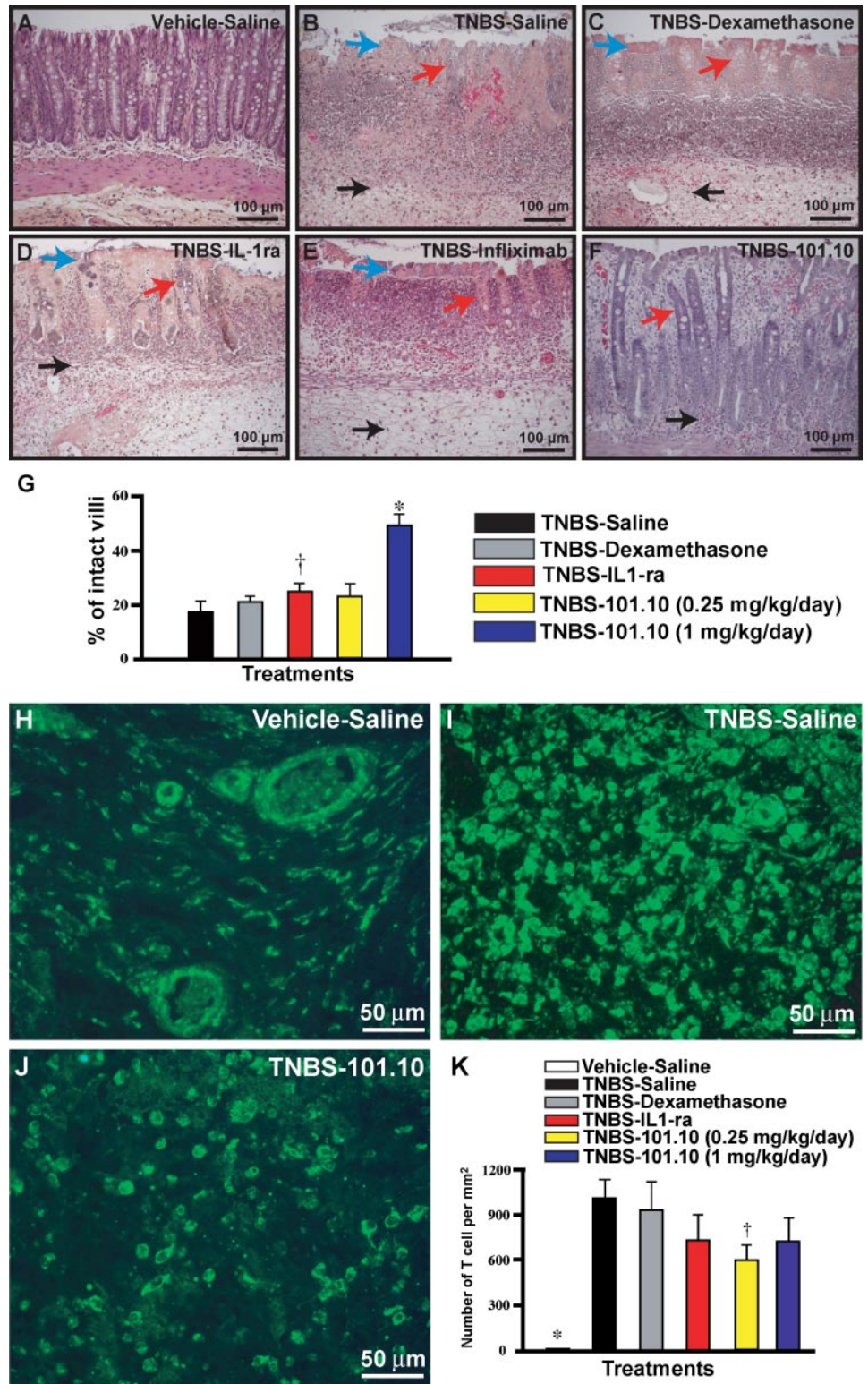
(43)) also diminished IL-1-induced hyperthermia (Fig. 5C). To ascertain that observed effects of 101.10 in vivo were not mediated via another relevant receptor, namely EP<sub>3</sub>, animals were treated with EP<sub>3</sub>-selective agonist PGE<sub>2</sub> analog M&B28767 (52) in absence and presence of 101.10. M&B28767-induced a comparable hyperthermia, which was unaffected by 101.10, consistent with in vitro selectivity of 101.10 (Figs. 3 and 5A).

IL-1 is also known to contribute to systemic hypotension secondary to bacterial endotoxins such as LPS (53). We tested the effects of 101.10 in wild-type and *IL-1RI*<sup>-/-</sup> animals. LPS caused a (maximum) 35% decrease in mean BP (MBP) of wild-type mice; 101.10 pretreatment attenuated the drop in MBP to 15% (Fig. 5D), without affecting baseline ( $\sim$ 100 mm Hg). *IL-1RI*<sup>-/-</sup> mice have a nearly identical baseline MBP to wild-type animals. In *IL-1RI*<sup>-/-</sup> mice LPS caused a decrease in MBP similar to that seen in 101.10-treated wild-type mice; 101.10 did not further affect MBP in *IL-1RI*-deficient animals treated with LPS (Fig. 5D). Data further substantiate in vivo specificity of 101.10.

#### *In vivo efficacy of 101.10 in animal models of inflammatory conditions*

IL-1 contributes significantly to numerous inflammatory conditions such as inflammatory bowel disease (54, 55) and contact dermatitis (56) including respectively in the TNBS-induced model of inflammatory bowel disease (57) and phorbol ester-induced dermatitis (58). Intracolonic TNBS caused pronounced inflammation of intestinal mucosa and submucosa at 48 h, as revealed by destruction of epithelium, crypts and submucosal region, associated with invasion of inflammatory cells (Fig. 6B). 101.10 dose-dependently improved preservation of intestinal integrity during this hyperacute phase of inflammatory destruction by TNBS, and its effects were significantly superior to dexamethasone (and equivalent to infliximab; Fig. 6G and Table II); the scrambled peptide was ineffective. Interestingly, focus on microscopic evaluation of villus integrity (the most important overall criteria) (Fig. 6G), T cell abundance (Fig. 6, H–K), and

**FIGURE 6.** Efficacy of 101.10 in TNBS model of inflammatory bowel disease. Sprague-Dawley rats were administered TNBS intrasigmoidal in absence or presence of ip treatment with saline (B), dexamethasone (0.75 mg/kg/day) (C), IL-1ra (8 mg/kg/day) (D), infliximab (10 mg/kg/day) (E), and 101.10 (1 mg/kg/day) (F) as compared with vehicle control (A). Animals were euthanized 48 h later and colons collected for macroscopic and histological examination. Representative histology is shown (A–F). Arrows point to following: epithelial denudation (blue arrows); crypt disruption (red arrows); neutrophil infiltration (black arrows). Values are mean ± SEM of three to eight experiments; \*†,  $p < 0.05$  compared with other values without same symbol. G, Quantification of intact intestinal villi normalized across total intestinal surface collected. H–J, Lymphocyte (CD4<sup>+</sup>) accumulation in intestinal tissue in normal and TNBS-exposed animals treated or not with 101.10. K, Quantification of T cell abundance in normal and TNBS-exposed tissues. Values are mean ± SEM of three to eight experiments; \*,  $p < 0.01$  compared with all other values; †,  $p < 0.05$  compared with TNBS with saline.



myeloperoxidase activity (which reflects neutrophil infiltration) (Table II), suggested superior efficacy of 101.10 (noncompetitive IL-1RI inhibitor; Fig. 4) over the competitive inhibitor IL-1ra (6); Fig. 6G). In addition, 12 h after administration of the proinflammatory irritant TNBS, systemic treatment with 101.10 was also found to diminish mucosal and submucosal destruction, albeit without affecting myeloperoxidase activity (Table II), likely because of insufficient time to clear invading neutrophils, which are however less cytotoxic during inhibition of

IL-1RI. Interestingly, pretreatment with intrarectal 101.10 (1 mg/kg/day) also attenuated the index of neutrophil invasion (myeloperoxidase activity) to  $56 \pm 9\%$  of control values ( $p < 0.05$ ).

Because of transepithelial (rectal) efficacy of 101.10 in TNBS-induced model of gut inflammation, we proceeded to verify the efficacy of topical 101.10 in a model of cutaneous inflammation induced by PMA; topical application of phorbol esters such as PMA induces an acute inflammatory reaction contributed by IL-1

Table II. Effect of 101.10 and other drug treatments on histologic evaluation of TNBS-induced colon inflammation in rat<sup>a</sup>

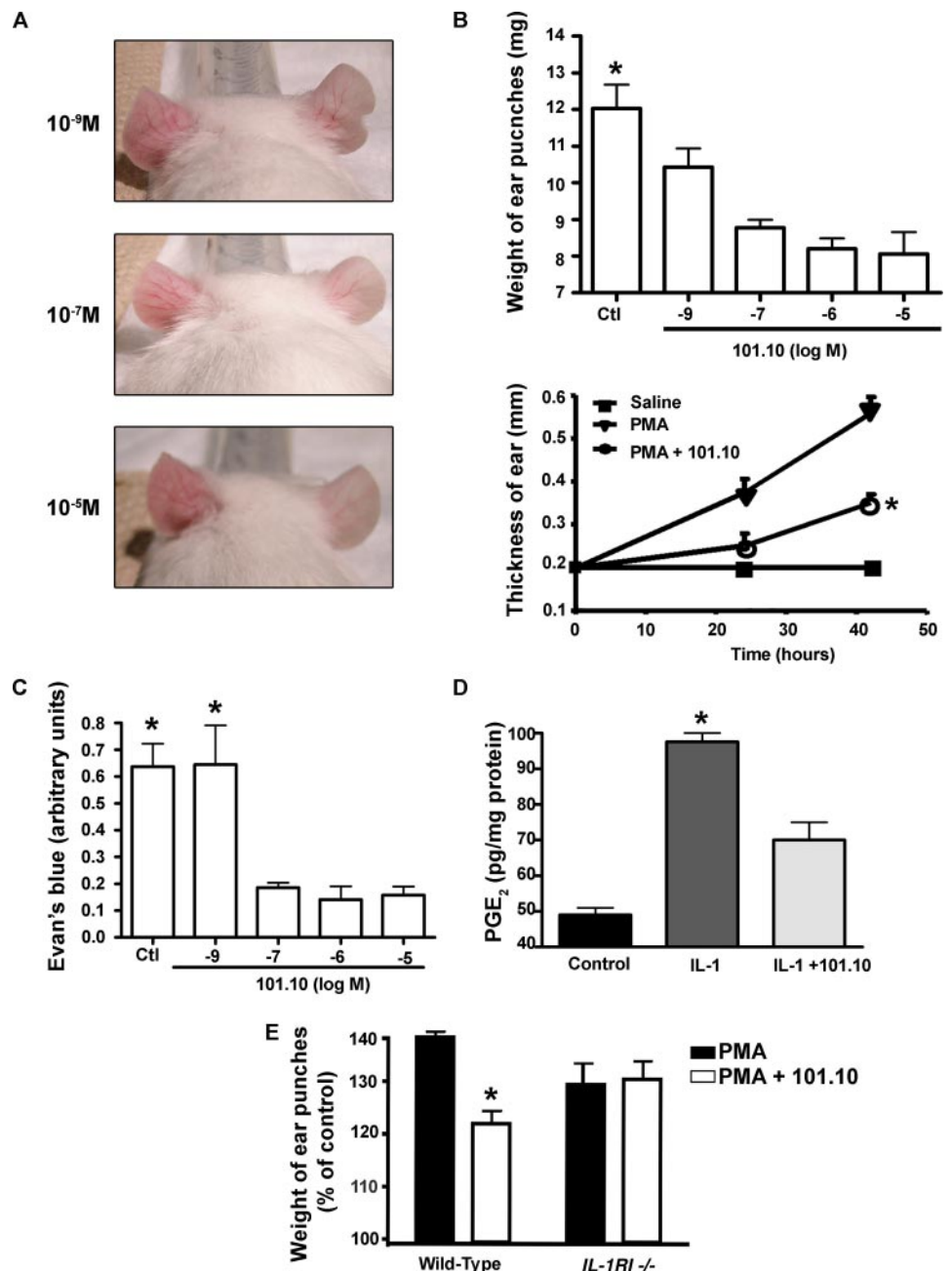
	Macroscopy (Score of 2)	Microscopy (Score of 5)	Myeloperoxidase (% of Control (TNBS))
Preventive Treatment			
TNBS ( <i>n</i> = 8)	1.57 ± 0.04	3.7 ± 0.2	100
+101.10 ( <i>n</i> = 8)	0.7 ± 0.1*	2.4 ± 0.3*	47 ± 7*
+IL-1ra ( <i>n</i> = 3)	0.84 ± 0.1*	2.0 ± 0.5*	63 ± 5*
+Infliximab ( <i>n</i> = 3)	0.87 ± 0.1*	2.4 ± 1.4*	60 ± 7*
+Dexamethasone ( <i>n</i> = 8)	ND	3.2 ± 0.3†	66 ± 18†
Treatment			
101.10 ( <i>n</i> = 7)	1.1 ± 0.1*	2.7 ± 0.1*	123 ± 18

<sup>a</sup> Macroscopy and microscopy scores are adapted from Peterson's scale (24). ND, not determined. Values are mean ± SEM. \*, *p* < 0.05 compared to TNBS alone; †, *p* < 0.05 compared to 101.10 (pretreatment).

(58). 101.10 (in PEG-400) applied twice a day to PMA-treated ears of CD-1 mice diminished dose- and time-dependently redness and edema formation measured by ear thickness and ear weight (esti-

mated EC<sub>50</sub> ≈ 10 nM; Fig. 7). These observations were consistent with a dose-dependent reduction in capillary extravasation (measured by Evan's Blue tissue concentration) and a decrease in tissue PGE<sub>2</sub>

**FIGURE 7.** Efficacy of topical 101.10 in PMA-induced dermatitis. CD-1 mice ears were treated either with PMA (0.05%, applied once daily) or PMA followed immediately with 101.10 mixed in PEG-400 (applied topically twice daily to contralateral ear). Ear thickness was measured throughout the experiment. At 42 h, animals were euthanized and 4-mm ear punches made and weighed; some animals were injected with Evan's blue to detect extravasation. **A**, Photographic representations of dose-dependent response to 101.10 applied to right ear; note marked reduction in redness of 101.10-treated right ears compared with untreated left ones. **B**, Time- and dose-dependent effect of 101.10 on ear weight and thickness of ear punches. **C**, Concentration-dependent effect of 101.10 on degree of capillary extravasation (measured by Evans blue in tissue). **D**, Efficacy of 101.10 (100 nM) on tissue PGE<sub>2</sub> concentrations. For **B–D**, values are mean ± SEM of three to five experiments; \*, *p* < 0.01 compared with values without asterisks. **E**, Effects of 101.10 (100 nM) on PMA-induced inflammatory edema in wild-type and *IL-1RI*<sup>-/-</sup> B6129S1 mice. 101.10 attenuated edema formation in wild-type but not in *IL-1RI*<sup>-/-</sup> mice, wherein edema is less pronounced than in wild-type congeners. Values are mean ± SEM percent of control (without PMA) of three to four experiments; \*, *p* < 0.01 compared with PMA in corresponding animal group.



concentrations (Fig. 7C); topical IL-1ra was ineffective (data not shown), as usually expected with proteins. Finally, parameters of PMA-induced edema (ear weight and thickness; latter not shown) were (as expected) diminished in *IL-1RI*<sup>-/-</sup> animals to levels approaching those after 101.10 in wild-type mice; 101.10 was ineffective in *IL-1RI*<sup>-/-</sup> animals (Fig. 7E).

## Discussion

Based on evidence that IL-1RacP interacts with the IL-1R subunit of the IL-1RI receptor complex (16) and that recombinant extracellular portion of IL-1RacP can interfere with IL-1RI actions (22), we designed peptides that reproduce various relevant IL-1RacP regions. Of these one small heptapeptide, termed "101.10," was found to be particularly effective in inhibiting IL-1-induced effects in vitro, although not necessarily fully (as seen with PGE<sub>2</sub>). 101.10 was a potent, selective, and reversible noncompetitive inhibitor of IL-1RI, and also exhibited modulatory properties, notably, by not interacting with the ligand binding (orthosteric) site, albeit by affecting IL-1-binding affinity and by interfering variably with different in vitro responses to IL-1. These features distinguish it from the large molecule competitive inhibitor IL-1ra (59). Consistent with IL-1-induced in vitro and in vivo (specifically hyperthermia) effects, 101.10 displayed effective anti-inflammatory capacity in acute inflammatory conditions involving IL-1. Findings describe a new small unprecedented noncompetitive antagonist of IL-1RI with valuable and increasingly desirable modulatory pharmacologic properties, consistent with those of an allosteric negative modulator that exhibits functional selectivity (7, 60–65).

The peptides we designed arose from loops and interdomain regions of the IL-1RacP (Fig. 1) and possess high flexibility profiles, enabling interaction with the IL-1RI subunit (16), which requires appropriate conformational changes. Primary sequence peptides reproducing specific protein regions have successfully been used to interfere with the effects of various receptors (8, 10–13, 66), and the effects of such peptides coincide with those of specific corresponding mutations (67, 68). Because these regions of interest are often remote from the natural ligand-binding site (orthosteric site), derived molecules are noncompetitive and can modulate ligand-binding affinity; these features are in line with characteristics of allosteric modulators (61, 69–71), and based on data presented, apply to 101.10. 101.10 binds specifically to IL-1R (including after cross-linking [11 Å]) but not to the IL-1-binding site, and accordingly is a noncompetitive antagonist (18, 19) of IL-1-induced effects (Figs. 3 and 4); because 101.10 appears to modulate (rather than totally interfere with) IL-1 binding to the IL-1RI (Fig. 4, D and E) which, in turn, facilitates complex formation with IL-1RacP (4), 101.10 can partly but not necessarily fully dissociate the complex, as suggested by cross-linking of [<sup>125</sup>I]101.10 to the IL-1RI/IL-1RacP complex (Fig. 3C). The noncompetitive property of 101.10 on IL-1-induced actions is further substantiated by the inability of increasing concentrations of IL-1 to overcome antagonist effects of 101.10 on IL-1-induced TF-1 proliferation, which is correspondingly reflected in plateauing of the Schild plot (Fig. 4A); in contrast, orthosteric antagonism by definition can be overcome by increasing concentrations of the natural ligand (88).

Another feature observed with allosteric modulators relates to their ability to modulate ligand-binding affinity; this was also seen with 101.10 which diminished binding affinity of IL-1 as revealed by the right shift of the curve of [<sup>125</sup>I]IL-1 displacement by IL-1 (Fig. 4D). The magnitude of change in both affinity and efficacy induced by such a receptor modulator is indicative of conformational modifications represented by the cooperativity constant  $\alpha$ —a measure of how the orthosteric and allosteric ligand perceive each other (65, 67, 72). Crystallographic analyses of protein complexes

often fail to detect small conformational changes ( $\leq 2$  Å), which may have profound effects on receptor function and are more readily appreciated by pharmacological binding and efficacy profiles (73). The  $\alpha$  constant for 101.10 to induce a two-fold shift of the IL-1-induced proliferation dose-response was positive but below a value of 1, which again suggests noncompetitive negative modulation on IL-1 potency toward its receptor (74). Altogether, one notes that 101.10 moderately decreases binding affinity of IL-1 but markedly depresses (some of) its function (Fig. 4); these observations contrast with those of orthosteric (competitive) inhibitors where changes in ligand binding somewhat correspond to those in function (60, 61, 75).

As alluded to above specific mutations (67, 76) or small molecules can affect some but not all functions evoked by a receptor (77–79). This property is referred to as pharmacological permissivity (7, 61, 65). This concept also appears to apply to 101.10, which partially inhibited IL-1-induced PGE<sub>2</sub> production but fully antagonized p38 (Fig. 2); this paradigm is further illustrated with peptides arising from other IL-1RacP regions (Fig. 1), namely 103, 106 and 108, which affected differently IL-1-induced PGE<sub>2</sub> and p38 phosphorylation (Fig. 2). This functional selectivity is made possible by ligands which bind in ways that affect the dynamic conformation of the receptor to interact with its natural ligand and associated proteins needed to activate normal signaling pathways (65, 74, 75); hence, such ligands can alter signaling modalities (18), which may confer greater selectivity (19) and reduce side effects (61), compared with orthosteric antagonists which disable all functions triggered by the receptor. These features seem to apply to 101.10 in line with what has lately been reported by other (noncytokine) receptors (77–80).

In agreement with its specific anti-IL-1RI actions in vitro, 101.10 exerted corresponding effects in vivo by curtailing IL-1-induced hyperthermia and hypotension (Fig. 5). Given the dominant role of IL-1 in acute bouts of inflammation a contribution for IL-1 in models of inflammatory conditions is also anticipated (1, 57, 58). Indeed, colon inflammation is characterized by a Th1 response, with high levels of IL-12, IL-6, IL-18, TNF- $\alpha$ , and IL-1, mostly produced by monocytes and macrophages (81, 82). In skin, IL-1 is mainly found in keratinocytes, fibroblasts, and endothelial cells, and is a sequestered pool ready to be released upon injury (83). 101.10 was effective in in vivo models of inflammatory conditions, as demonstrated in two distinct models of inflammation induced in gut by TNBS and on cutaneous tissue by PMA (Table II; Figs. 6 and 7), consistent with reported efficacy of IL-1ra in analogous models (84–87). In contrast to genetically intact animals, 101.10 was ineffective on IL-1-dependent physiologic and inflammatory parameters induced in *IL-1RI*<sup>-/-</sup> mice (Figs. 5 and 7), consistent with its specificity (Figs. 3 and 5).

In summary, we hereby document the discovery and pharmacological properties of a small stable (D-) peptide antagonist of IL-1RI, namely 101.10, which is rationally derived from an extracellular loop region of IL-1RacP (see Fig. 1) and exhibits properties consistent with those of an allosteric negative modulator. As a competitive inhibitor of IL-1, IL-1ra interferes with all actions of IL-1RI, including desirable ones related to innate immunity, and hence increases the risk of cancer and seemingly of infections (85). In this report, we have described the first small molecule (peptide) antagonist of a cytokine receptor, notably of *IL-1RI*, which seems to integrate allosteric modulatory properties; 101.10 is specific, potent and effective in vitro and in vivo in (IL-1-implicated) models of inflammation after systemic and topical applications. Because 101.10 appears to some extent more effective than the competitive antagonist IL-1ra in in vivo inflammatory conditions (Table II and Fig. 6), 101.10 (and small like-compounds) could

present therapeutic benefits, including those pertaining to simpler modes of administration (e.g., transepithelial; Fig. 7), and likely costs; moreover pharmacologically, they expose new and interesting properties (notably functional selectivity) in countering undesired exaggerated IL-1-elicited inflammation.

## Acknowledgments

We thank Hendrika Fernandez for technical assistance.

## Disclosures

The authors have no financial conflict of interest.

## References

- McCulloch, C. A., G. P. Downey, and H. El-Gabalawy. 2006. Signalling platforms that modulate the inflammatory response: new targets for drug development. *Nat. Rev. Drug Discov.* 5: 864–876.
- Kavanaugh, A. 2006. Anakinra (interleukin-1 receptor antagonist) has positive effects on function and quality of life in patients with rheumatoid arthritis. *Adv. Ther.* 23: 208–217.
- Mee, J. B., M. J. Cork, F. S. di Giovine, G. W. Duff, and R. W. Groves. 2006. Interleukin-1: a key inflammatory mediator in psoriasis? *Cytokine* 33: 72–78.
- Dower, S. K., J. E. Sims, T. H. Stanton, J. Slack, C. J. McMahan, M. A. Valentine, and K. Bomszyk. 1990. Molecular heterogeneity of interleukin-1 receptors. *Ann. NY Acad. Sci.* 594: 231–239.
- Dinarello, C. A., S. Gatti, and T. Bartfai. 1999. Fever: links with an ancient receptor. *Curr. Biol.* 9: R147–150.
- Arend, W. P. 1993. Interleukin-1 receptor antagonist. *Adv. Immunol.* 54: 167–227.
- Urban, J. D., W. P. Clarke, M. von Zastrow, D. E. Nichols, B. Kobilka, H. Weinstein, J. A. Javitch, B. L. Roth, A. Christopoulos, P. M. Sexton, et al. 2007. Functional selectivity and classical concepts of quantitative pharmacology. *J. Pharmacol. Exp. Ther.* 320: 1–13.
- Zhou, N., Z. Luo, J. Luo, X. Fan, M. Hiraoka, D. Liu, X. Han, J. Pesavento, C. Z. Dong, et al. 2002. Exploring the stereochemistry of CXCR4-peptide recognition and inhibiting HIV-1 entry with D-peptides derived from chemokines. *J. Biol. Chem.* 277: 17476–17485.
- McDonnell, J. M., A. J. Beavil, G. A. Mackay, B. A. Jameson, R. Korngold, H. J. Gould, and B. J. Sutton. 1996. Structure based design and characterization of peptides that inhibit IgE binding to its high-affinity receptor. *Nat. Struct. Biol.* 3: 419–426.
- Chalifour, R. J., R. W. McLaughlin, L. Lavoie, C. Morissette, N. Tremblay, M. Boule, P. Sarazin, D. Stea, D. Lacombe, P. Tremblay, and F. Gervais. 2003. Stereoselective interactions of peptide inhibitors with the  $\beta$ -amyloid peptide. *J. Biol. Chem.* 278: 34874–34881.
- Zhang, T. T., B. Cui, D. Z. Dai, and X. Y. Tang. 2005. Pharmacological efficacy of CPU 86017 on hypoxic pulmonary hypertension in rats: mediated by direct inhibition of calcium channels and antioxidant action, but indirect effects on the ET-1 pathway. *J. Cardiovasc. Pharmacol.* 46: 727–734.
- Peri, K. G., C. Quiniou, X. Hou, D. Abran, D. R. Varma, W. D. Lubell, and S. Chemtob. 2002. THG113: a novel selective FP antagonist that delays preterm labor. *Semin. Perinatol.* 26: 389–397.
- Hebert, T. E., S. Moffett, J. P. Morello, T. P. Loisel, D. G. Bichet, C. Barret, and M. Bouvier. 1996. A peptide derived from a  $\beta$ 2-adrenergic receptor transmembrane domain inhibits both receptor dimerization and activation. *J. Biol. Chem.* 271: 16384–16392.
- Gusic, R. J., M. Petko, R. Myung, J. William Gaynor, and K. J. Gooch. 2005. Mechanical properties of native and ex vivo remodeled porcine saphenous veins. *J. Biomech.* 38: 1770–1779.
- Slingsby, C., O. A. Bateman, and A. Simpson. 1993. Motifs involved in protein-protein interactions. *Mol. Biol. Rep.* 17: 185–195.
- Casadio, R., E. Frigimelica, P. Bossu, D. Neumann, M. U. Martin, A. Tagliabue, and D. Boraschi. 2001. Model of interaction of the IL-1 receptor accessory protein IL-1RAcP with the IL-1 $\beta$ /IL-1R(I) complex. *FEBS Lett.* 499: 65–68.
- Tan, D. C., R. M. Kini, S. D. Jois, D. K. Lim, L. Xin, and R. Ge. 2001. A small peptide derived from Flt-1 (VEGFR-1) functions as an angiogenic inhibitor. *FEBS Lett.* 494: 150–156.
- Presland, J. 2005. Identifying novel modulators of G protein-coupled receptors via interaction at allosteric sites. *Curr. Opin. Drug Discov. Devel.* 8: 567–576.
- Lazareno, S. 2004. Determination of allosteric interactions using radioligand-binding techniques. *Methods Mol. Biol.* 259: 29–46.
- Murali, R., X. Cheng, A. Berezov, X. Du, A. Schon, E. Freire, X. Xu, Y. H. Chen, and M. I. Greene. 2005. Disabling TNF receptor signaling by induced conformational perturbation of tryptophan-107. *Proc. Natl. Acad. Sci. USA* 102: 10970–10975.
- Anderson, M. E., B. A. Tejo, T. Yakovleva, and T. J. Siahaan. 2006. Characterization of binding properties of ICAM-1 peptides to LFA-1: inhibitors of T-cell adhesion. *Chem. Biol. Drug Des.* 68: 20–28.
- Smeets, R. L., L. A. Joosten, O. J. Arntz, M. B. Bennink, N. Takahashi, H. Carlsen, M. U. Martin, W. B. van den Berg, and F. A. van de Loo. 2005. Soluble interleukin-1 receptor accessory protein ameliorates collagen-induced arthritis by a different mode of action from that of interleukin-1 receptor antagonist. *Arthritis Rheum.* 52: 2202–2211.
- Labow, M., D. Shuster, M. Zetterstrom, P. Nunes, R. Terry, E. B. Cullinan, T. Bartfai, C. Solorzano, L. L. Moldawer, R. Chizzonite, and K. W. McIntyre. 1997. Absence of IL-1 signaling and reduced inflammatory response in IL-1 type I receptor-deficient mice. *J. Immunol.* 159: 2452–2461.
- Vigers, G. P., L. J. Anderson, P. Caffes, and B. J. Brandhuber. 1997. Crystal structure of the type-I interleukin-1 receptor complexed with interleukin-1 $\beta$ . *Nature* 386: 190–194.
- Boeckmann, B., A. Bairoch, R. Apweiler, M. C. Blatter, A. Estreicher, E. Gasteiger, M. J. Martin, K. Michoud, C. O'Donovan, I. Phan, et al. 2003. The SWISS-PROT protein knowledgebase and its supplement TrEMBL in 2003. *Nucleic Acids Res.* 31: 365–370.
- Rost, B., P. Fariselli, and R. Casadio. 1996. Topology prediction for helical transmembrane proteins at 86% accuracy. *Protein Sci.* 5: 1704–1718.
- Kyte, J., and R. F. Doolittle. 1982. A simple method for displaying the hydrophobic character of a protein. *J. Mol. Biol.* 157: 105–132.
- Isbil-Buyukcoskun, N., G. Gulec, K. Ozluk, and I. H. Ulus. 2001. Central injection of captopril inhibits the blood pressure response to intracerebroventricular choline. *Braz. J. Med. Biol. Res.* 34: 815–820.
- Brault, S., A. K. Martinez-Bermudez, A. M. Marrache, F. Gobeil, Jr., X. Hou, M. Beauchamp, C. Quiniou, G. Almazan, C. Lachance, J. Roberts, Jr., et al. 2003. Selective neuromicrovascular endothelial cell death by 8-iso-prostaglandin F $_{2\alpha}$ : possible role in ischemic brain injury. *Stroke* 34: 776–782.
- Peterson, T. C., C. E. Cleary, A. M. Shaw, D. A. Malatjalian, and S. J. Veldhuyzen van Zanten. 2000. Therapeutic role for bismuth compounds in TNBS-induced colitis in the rat. *Dig. Dis. Sci.* 45: 466–473.
- Strober, W. 1985. Animal models of inflammatory bowel disease: an overview. *Dig. Dis. Sci.* 30: 3S–10S.
- Stein, J., J. Ries, and K. E. Barrett. 1998. Disruption of intestinal barrier function associated with experimental colitis: possible role of mast cells. *Am. J. Physiol.* 274: G203–G209.
- Sandberg, J. O., D. L. Eizirik, and S. Sandler. 1997. IL-1 receptor antagonist inhibits recurrence of disease after syngeneic pancreatic islet transplantation to spontaneously diabetic non-obese diabetic (NOD) mice. *Clin. Exp. Immunol.* 108: 314–317.
- Zwerina, J., S. Hayer, M. Tohidast-Akrad, H. Bergmeister, K. Redlich, U. Feige, C. Dunstan, G. Kollias, G. Steiner, J. Smolen, and G. Schett. 2004. Single and combined inhibition of tumor necrosis factor, interleukin-1, and RANKL pathways in tumor necrosis factor-induced arthritis: effects on synovial inflammation, bone erosion, and cartilage destruction. *Arthritis Rheum.* 50: 277–290.
- Krawisz, J. E., P. Sharon, and W. F. Stenson. 1984. Quantitative assay for acute intestinal inflammation based on myeloperoxidase activity: assessment of inflammation in rat and hamster models. *Gastroenterology* 87: 1344–1350.
- Nadeau, S., and S. Rivest. 2002. Endotoxemia prevents the cerebral inflammatory wave induced by intraparenchymal lipopolysaccharide injection: role of glucocorticoids and CD14. *J. Immunol.* 169: 3370–3381.
- Tomonari, K. 1988. A rat antibody against a structure functionally related to the mouse T-cell receptor/T3 complex. *Immunogenetics* 28: 455–458.
- Rauschmayr, T., R. W. Groves, and T. S. Kupper. 1997. Keratinocyte expression of the type 2 interleukin 1 receptor mediates local and specific inhibition of interleukin 1-mediated inflammation. *Proc. Natl. Acad. Sci. USA* 94: 5814–5819.
- Wamberg, S., N. C. Sandgaard, and P. Bie. 2002. Simultaneous determination of total body water and plasma volume in conscious dogs by the indicator dilution principle. *J. Nutr.* 132: 1711S–1713S.
- Dombrowicz, D., V. Flamand, I. Miyajima, J. V. Ravetch, S. J. Galli, and J. P. Kinet. 1997. Absence of Fc $\epsilon$ R1  $\alpha$  chain results in upregulation of Fc $\gamma$ RIII-dependent mast cell degranulation and anaphylaxis: evidence of competition between Fc $\epsilon$ R1 and Fc $\gamma$ RIII for limiting amounts of FcR  $\beta$  and  $\gamma$  chains. *J. Clin. Invest.* 99: 915–925.
- Gobeil, F., A. Fortier, T. Zhu, M. Bossolasco, M. Leduc, M. Grandbois, N. Heveker, G. Bkaily, S. Chemtob, and D. Barbaz. 2006. G-protein-coupled receptors signalling at the cell nucleus: an emerging paradigm. *Can. J. Physiol. Pharmacol.* 84: 287–297.
- Fan, L., W. V. Yotov, T. Zhu, L. Esmailzadeh, J. S. Joyal, F. Sennlaub, N. Heveker, S. Chemtob, and G. E. Rivard. 2005. Tissue factor enhances protease-activated receptor-2-mediated factor VIIa cell proliferative properties. *J. Thromb. Haemost.* 3: 1056–1063.
- Li, D. Y., P. Hardy, D. Abran, A. K. Martinez-Bermudez, A. M. Guerguerian, M. Bhattacharya, G. Almazan, R. Menezes, K. G. Peri, D. R. Varma, and S. Chemtob. 1997. Key role for cyclooxygenase-2 in PGE $_2$  and PGF $_{2\alpha}$  receptor regulation and cerebral blood flow of the newborn. *Am. J. Physiol.* 273: R1283–R1290.
- Banks, W. A. 1999. Characterization of interleukin-1 $\alpha$  binding to mouse brain endothelial cells. *J. Pharmacol. Exp. Ther.* 291: 665–670.
- Marrache, A. M., F. Gobeil, Jr., S. G. Bernier, J. Stankova, M. Rola-Pleszczynski, S. Choufani, G. Bkaily, A. Bourdeau, M. G. Sirois, A. Vazquez-Tello, et al. 2002. Proinflammatory gene induction by platelet-activating factor mediated via its cognate nuclear receptor. *J. Immunol.* 169: 6474–6481.
- Takeuchi, M., S. Nagai, H. Nakada, H. Aung, N. Satake, H. Kaneshima, and T. Izumi. 1992. Characterization of IL-1 inhibitory factor released from human alveolar macrophages as IL-1 receptor antagonist. *Clin. Exp. Immunol.* 88: 181–187.
- Howe, R. C., J. W. Lowenthal, and H. R. MacDonald. 1986. Role of interleukin 1 in early T cell development: Lyt-2-L3T4 $^+$  thymocytes bind and respond in vitro to recombinant IL 1. *J. Immunol.* 137: 3195–3200.
- Cox, G. W., B. J. Mathieson, S. L. Giardino, and L. Varesio. 1990. Characterization of IL-2 receptor expression and function on murine macrophages. *J. Immunol.* 145: 1719–1726.

49. Gao, Z. G., S. K. Kim, A. P. Ijzerman, and K. A. Jacobson. 2005. Allosteric modulation of the adenosine family of receptors. *Mini. Rev. Med. Chem.* 5: 545–553.
50. Lazarus, M. 2006. The differential role of prostaglandin E2 receptors EP3 and EP4 in regulation of fever. *Mol. Nutr. Food Res.* 50: 451–455.
51. Romanovsky, A. A., M. C. Almeida, D. M. Aronoff, A. I. Ivanov, J. P. Konsman, A. A. Steiner, and V. F. Turek. 2005. Fever and hypothermia in systemic inflammation: recent discoveries and revisions. *Front. Biosci.* 10: 2193–2216.
52. Boie, Y., R. Stocco, N. Sawyer, D. M. Slipetz, M. D. Ungrin, F. Neuschaefer-Rube, G. P. Puschel, K. M. Metters, and M. Abramovitz. 1997. Molecular cloning and characterization of the four rat prostaglandin E2 prostanoid receptor subtypes. *Eur. J. Pharmacol.* 340: 227–241.
53. Gardiner, S. M., P. A. Kemp, J. E. March, J. Woolley, and T. Bennett. 1998. The influence of antibodies to TNF- $\alpha$  and IL-1 $\beta$  on haemodynamic responses to the cytokines, and to lipopolysaccharide, in conscious rats. *Br. J. Pharmacol.* 125: 1543–1550.
54. Rogler, G., and T. Andus. 1998. Cytokines in inflammatory bowel disease. *World J. Surg.* 22: 382–389.
55. Maeda, S., L. C. Hsu, H. Liu, L. A. Bankston, M. Iimura, M. F. Kagnoff, L. Eckmann, and M. Karin. 2005. Nod2 mutation in Crohn's disease potentiates NF- $\kappa$ B activity and IL-1 $\beta$  processing. *Science* 307: 734–738.
56. Corsini, E., and C. L. Galli. 1998. Cytokines and irritant contact dermatitis. *Toxicol. Lett.* 102–103: 277–282.
57. Galvez, J., M. Garrido, M. E. Rodriguez-Cabezas, I. Ramis, F. S. de Medina, M. Merlos, and A. Zarzuelo. 2003. The intestinal anti-inflammatory activity of UR-12746S on reactivated experimental colitis is mediated through downregulation of cytokine production. *Inflamm. Bowel Dis.* 9: 363–371.
58. Ha, H. Y., Y. Kim, Z. Y. Ryoo, and T. Y. Kim. 2006. Inhibition of the TPA-induced cutaneous inflammation and hyperplasia by EC-SOD. *Biochem. Biophys. Res. Commun.* 348: 450–458.
59. Carter, D. B., M. R. Deibel, Jr., C. J. Dunn, C. S. Tomich, A. L. Laborde, J. L. Slightom, A. E. Berger, M. J. Bienkowski, F. F. Sun, R. N. McEwan, et al. 1990. Purification, cloning, expression and biological characterization of an interleukin-1 receptor antagonist protein. *Nature* 344: 633–638.
60. Kenakin, T., and O. Onaran. 2002. The ligand paradox between affinity and efficacy: can you be there and not make a difference? *Trends Pharmacol. Sci.* 23: 275–280.
61. Kenakin, T. 2004. Allosteric modulators: the new generation of receptor antagonist. *Mol. Interv.* 4: 222–229.
62. Kenakin, T. 2004. G-protein coupled receptors as allosteric machines. *Receptors Channels* 10: 51–60.
63. Kenakin, T. 2004. Principles: receptor theory in pharmacology. *Trends Pharmacol. Sci.* 25: 186–192.
64. Kenakin, T. 2004. Efficacy as a vector: the relative prevalence and paucity of inverse agonism. *Mol. Pharmacol.* 65: 2–11.
65. Kenakin, T. 2005. New concepts in drug discovery: collateral efficacy and permissive antagonism. *Nat. Rev. Drug Discov.* 4: 919–927.
66. Gonzalez-Ruiz, D., and H. Gohlke. 2006. Targeting protein-protein interactions with small molecules: challenges and perspectives for computational binding epitope detection and ligand finding. *Curr. Med. Chem.* 13: 2607–2625.
67. May, L. T., K. Leach, P. M. Sexton, and A. Christopoulos. 2007. Allosteric modulation of G protein-coupled receptors. *Annu. Rev. Pharmacol. Toxicol.* 47: 1–51.
68. Miedlich, S. U., L. Gama, K. Seuwen, R. M. Wolf, and G. E. Breitwieser. 2004. Homology modeling of the transmembrane domain of the human calcium sensing receptor and localization of an allosteric binding site. *J. Biol. Chem.* 279: 7254–7263.
69. Kenakin, T., S. Jenkinson, and C. Watson. 2006. Determining the potency and molecular mechanism of action of insurmountable antagonists. *J. Pharmacol. Exp. Ther.* 319: 710–723.
70. Lukong, K. E., M. A. Elsliger, J. S. Mort, M. Potier, and A. V. Pshzhetsky. 1999. Identification of UDP-N-acetylglucosamine-phosphotransferase-binding sites on the lysosomal proteases, cathepsins A, B, and D. *Biochemistry* 38: 73–80.
71. Xie, Y., S. M. Massa, S. E. Ensslen-Craig, D. L. Major, T. Yang, M. A. Tisi, V. D. Derevyanny, W. O. Runge, B. P. Mehta, L. A. Moore, et al. 2006. Protein-tyrosine phosphatase (PTP) wedge domain peptides: a novel approach for inhibition of PTP function and augmentation of protein-tyrosine kinase function. *J. Biol. Chem.* 281: 16482–16492.
72. Ehlert, F. J. 2005. Analysis of allosterism in functional assays. *J. Pharmacol. Exp. Ther.* 315: 740–754.
73. Koshland, D. E., Jr. 1998. Conformational changes: how small is big enough? *Nat. Med.* 4: 1112–1114.
74. Christopoulos, A. 2002. Allosteric binding sites on cell-surface receptors: novel targets for drug discovery. *Nat. Rev. Drug. Discov.* 1: 198–210.
75. Christopoulos, A., L. T. May, V. A. Avlani, and P. M. Sexton. 2004. G-protein-coupled receptor allosterism: the promise and the problem(s). *Biochem. Soc. Trans* 32: 873–877.
76. Hemstapat, K., M. T. Smith, and G. R. Monteith. 2004. Measurement of intracellular Ca<sup>2+</sup> in cultured rat embryonic hippocampal neurons using a fluorescence microplate reader: potential application to biomolecular screening. *J. Pharmacol. Toxicol. Methods* 49: 81–87.
77. Maillet, E. L., N. Pellegrini, C. Valant, B. Bucher, M. Hibert, J. J. Bourguignon, and J. L. Galzi. 2007. A novel, conformation-specific allosteric inhibitor of the tachykinin NK2 receptor (NK2R) with functionally selective properties. *FASEB J.* 21: 2124–2134.
78. Rodriguez, A. L., Y. Nong, N. K. Sekaran, D. Alagille, G. D. Tamagnan, and P. J. Conn. 2005. A close structural analog of 2-methyl-6-(phenylethynyl)-pyridine acts as a neutral allosteric site ligand on metabotropic glutamate receptor subtype 5 and blocks the effects of multiple allosteric modulators. *Mol. Pharmacol.* 68: 1793–1802.
79. Lysikova, M., Z. Havlas, and S. Tucek. 2001. Interactions between allosteric modulators and 4-DAMP and other antagonists at muscarinic receptors: potential significance of the distance between the N and carboxyl C atoms in the molecules of antagonists. *Neurochem. Res.* 26: 383–394.
80. Litschig, S., F. Gasparini, D. Rueegg, N. Stoehr, P. J. Flor, I. Vranesic, L. Prezeau, J. P. Pin, C. Thomsen, and R. Kuhn. 1999. CPCCOEt, a noncompetitive metabotropic glutamate receptor 1 antagonist, inhibits receptor signaling without affecting glutamate binding. *Mol. Pharmacol.* 55: 453–461.
81. Neurath, M. F. 2000. Immunotherapy of inflammatory bowel diseases: current concepts and future perspectives. *Arch. Immunol. Ther. Exp.* 48: 81–84.
82. Kim, H. S., and A. Berstad. 1992. Experimental colitis in animal models. *Scand. J. Gastroenterol.* 27: 529–537.
83. Hauser, C., J. H. Saurat, A. Schmitt, F. Jaunin, and J. M. Dayer. 1986. Interleukin 1 is present in normal human epidermis. *J. Immunol.* 136: 3317–3323.
84. Kondo, S., B. P. Barna, T. Morimura, J. Takeuchi, J. Yuan, A. Akbasak, and G. H. Barnett. 1995. Interleukin-1  $\beta$ -converting enzyme mediates cisplatin-induced apoptosis in malignant glioma cells. *Cancer Res.* 55: 6166–6171.
85. Kondo, S., S. Pastore, H. Fujisawa, G. M. Shivji, R. C. McKenzie, C. A. Dinarello, and D. N. Sauder. 1995. Interleukin-1 receptor antagonist suppresses contact hypersensitivity. *J. Invest. Dermatol.* 105: 334–338.
86. Zhu, F., J. Qian, G. Pan, and S. Quan. 1998. The effect of interleukin-1  $\beta$  interleukin-8 in the pathogenesis of experimental colitis and evaluation of interleukin-1 receptor antagonist therapy. *Zhongguo Yi Xue Ke Xue Yuan Xue Bao* 20: 388–394.
87. Ricci, S., G. Macchia, P. Ruggiero, T. Maggi, P. Bossu, L. Xu, D. Medaglini, A. Tagliabue, L. Hammarstrom, G. Pozzi, and D. Boraschi. 2003. In vivo mucosal delivery of bioactive human interleukin 1 receptor antagonist produced by *Streptococcus gordonii*. *BMC Biotechnol.* 3: 15.
88. Matthews, J. C. 1993. *Fundamentals of Receptor, Enzyme, and Transport Kinetics*, 1st Ed. CRC Press, Boca Raton, FL, pp. 63–94.